



45 comprehensive analysis was performed on the lithological, petrographic, and
46 geomorphological data from the upper stratum of Quaternary sediments of the column. Based
47 on the shape and morphology of quartz grains, some features of glacial processes for some
48 layers of the studied sections were identified and analysed with special attention to the
49 environmental history. A petrographic study of the boulder samples was carried out, which
50 showed that the majority of samples are boulders of glacial origin according to their shape
51 and texture. For the first time, digital terrain models were applied to study of the key plot
52 where the lithological column is situated, which made it possible to identify the specific
53 terrain areas that were most likely formed by glaciation. It is suggested that extensive
54 lacustrine-alluvial plains existed in the Nadym River Basin, which was represented by
55 postglacial sites. Such a concept provides a lithological basis for understanding the reasons
56 for the formation of the present and recently formed environments and landforms. Therefore,
57 it could be possible that local glaciation in the region of the Nadym River's lower course had
58 an effect on the formation of the stratification of the layers of Quaternary origin.
59

60 1. Introduction

61 The history of geomorphology development in the northern part of Western Siberia has
62 been a subject of intensive discussion during the last part of XX-th century. The stratigraphy
63 of Enisey river estuary is a key factor of West-Siberian lowland quaternary evolution. The
64 problem of the presence and distribution of cover glaciations in the Pleistocene is the most
65 problematic for current geomorphology of North part of Western Siberia. Numerous
66 examples of sedimentation alternation, induced by various cover glaciations of different ages
67 and thicknesses are presented here in different geomorphological levels and landforms. These
68 series of sediments has been used as a background reference points for geological
69 interpretation of the history of Western-Siberian lowland. A certain compromise between the
70 opposite point of views on glaciation presence on the territory of Western Siberia was
71 proposed by scientists of the Tyumen complex expedition of the geographical faculty of
72 Moscow State University, who prepared in 1971 Atlas of the Tyumen region. G.I. Lazukov
73 and M.E. Gorodetskaya developed a geomorphological regionalization scheme, which shows
74 limited areas of maximum Samara glaciation along the periphery of Western Siberia without
75 formation of a single ice shield, while the main territory is presented in the form of a series of
76 different-altitude sea terraces of different degree of dismemberment (Lazukov, 1972).
77 Numerous discussions at geological plenary and commissions did not lead to the formation of
78 a single representation, so the second edition of the Q-42-43 of the State Geological map of
79 scale 1:1000000 (an edition S.B. Shatsky, 1995). Thus, a number of contradictions at the
80 general prevalence of the glacial concept contains - on the map simultaneously with glacial,
81 fluvial and glacial deposits are specified marine and glaciomarine, borders of large stages the
82 late Pleistocene of gaciations are allocated. At the present stage (including the period from
83 the second half of the 1990s) with the general reduction of geological surveys intensity, the
84 work on harmonization of contradictory points of view was continued. In 1999, the Legend of
85 the Tyumen-Salekhard Subseries of the West Siberian Series map was approved to the sheets
86 of Gosgeological map-200, based on a stratigraphic approach, which allows to more
87 objectively dismount and correlate cuts on the basis of complex paleogeomorphological
88 analysis taking into account the results of all available methods of research (paleontological,
89 physical, first of all paleomagenic).

90 The state geological map of Russia Q-43 for this region indicates the dominance of
91 glacial and fluvioglacial types of the surface sediments (Alyavdin, Mokin, 1957). The
92 possible existence of ice sheets and related permafrost sediments was identified as a key issue



93 in the beginning of the systematic geological study of this territory in the 1960s. Some
94 researchers (e.g., Svendsen, 2004) have suggested that there were extended glaciations that
95 resulted in blocking of the river or parts of rivers at certain stages, leading to the formation of
96 large glacier-dammed lakes (Grosvald, 1999). Another point of view is related to the possible
97 existence of glaciation on the plain (Generalov, 1986). That is why the landforms present as a
98 sequence of terraces formed by marine transgressions of various ages. There is also an
99 opinion that the glaciation was localized in the form of ice caps on separate watersheds and
100 that the river flow unblocked (Velichko, 1987; Velichko et al., 1997). Bolshiyarov (2006)
101 have argued this opinion and have implemented the term “passive glaciation”. In this context,
102 it is assumed, that the sea level fluctuations might have created extended abrasion platforms.
103 Also, there is a point of view that those forms of relief, which previously were considered as
104 glacial and fluvio-glacial (morains and eskers) were not originated from cover glaciations,
105 but resulted from erosion, abrasion and thermokarst outcrops related to permafrost-erosion
106 and tectonic processes of the late Pleistocene. It was suggested, that isolated parts of
107 Smarovskoye glaciation was presented in some parts of the Tyumen region in combination
108 with relics of ancient marine terraces (Lazukov, 1972). Later, the intensive discussion was
109 between geologists regarding the nature of possible glaciations and sedimentation history on
110 the territory of Western Siberia. It was suggested that glaciations has been extended till
111 Siberian ridges where it was continued by ancient periglacial Mansyiskoye lake (Grosvald,
112 1999). Bolshiyarov (2006) suggested that the glaciations was passive, without formation of
113 discontinuous cover and without blocking of the preferential flow in topography. At the same
114 time, the abrasion relief with extended ledges has been formed in late Pleistocene period.
115 In the region of Nadym river the investigations of sediments stratigraphy and landforms
116 development was started in 1960-th. As result of theses, works 3 generation of geological
117 maps were created. Here, there numerous geomorphological levels are presented. But, this
118 region was not covered by Russian-Norwegian project “Queen”. It was suggested on the sheet
119 of the state geological map Q-42-43 that there is a combination of glacial and marine glacial
120 sediments and numerous lake terraces on the territory of Western Siberia. Nowadays, the
121 glacial sediments are excluded from the current version of the state geological map
122 (Babushkin, 1995) which is in contradiction to the results, obtained by Zastrozhnov (2011)
123 and Fredin et al. (2012). Nowadays, there is not uniform concept of the landforms genesis in
124 Western Siberia. The basing of the Nadym river is considered as most important for
125 quaternary interpretation of this region history in Pleistocene. The topography and sediments
126 of the Nadym River is one of the most informative key territories where numerous field
127 investigations and remote sensing operations have carried out by numerous generations of
128 researchers. The results of studying the Nadym River and adjacent areas, among other data,
129 have served as a basis for classification of the Quaternary deposits in West Siberia
130 (Maslennikov, 1998, Sedov et al, 2016, Sheinkman et al, 2016, Rusakov et al, 2018).
131 Sheinkmann et al (2016) use to deny the presence of glaciation and their role in landform
132 formation. In opposite, Bolshiyarov (2006) suggest that glaciation has existed and was
133 important for geomorphological history of the surrounding of Nadym river. Nevertheless, the
134 current geological map (Faibusovic, Abakumova, 2015) involves unsolved issues that are
135 manifesting as new geological and geomorphologic data obtained. Thus, the objective of this
136 study is to conduct detailed lithological, petrographic and geomorphologic analyses in the
137 lower course the Nadym River with special reference to indicators of the key factors,
138 affecting the sedimentation and landform formations.
139



140 2. Materials and methods

141 2.1 The study sites

142 The field investigations were carried out in August 2016 on the left bank of the Nadym
143 River near the confluence of the Kheigiyakha (Long Ugan) River, 40 km south-west of the
144 city of Nadym (Yamalo-Nenets Autonomous Okrug, Russia). The area is well developed in
145 terms of industry and includes main gas lines (the Urengoi–Pomary–Uzhhorod line, Nadym–
146 Punga–Nizhnyaya Tura line, etc.), high-voltage power transmission lines (200 kV, 500 kV),
147 an oil pipeline (CPF Yarudeyskoye oil field – OPS Purpe), and a hard-surface motorway
148 (Nadym–Yagelnoye Road). Due to the lack of natural exposures, two quarries were chosen
149 for this research (N65.350455°, E72.970881°, and N65.061417°, E72.943848°). Two
150 sections were made in the quarry walls: K-1 and K-2, which are 5 m and 6 m high,
151 respectively (Fig. 1). The area selected it best example for investigation Quaternary history in
152 central part of Yamal region due to geomorphological peculiarities and stratification.

153 The vertical sections were exposed on the high bank of the Nadym River. Sections K-1
154 and K-2 show the structure of a second terrace above the floodplain of the Nadym and
155 Levaya Khetta Rivers. Section K-1 was made in the eastern wall of sand quarry N1 within the
156 Aeolian massif (N65.350455°, E72.970881°, absolute elevation 20 m). The total thickness of
157 the exposed stratum was 435 cm. A detailed description of each horizon is given in Table 1,
158 and a general view of the section is shown in Figure 2(a).

159 Section K-2 was made in the northern wall of dormant sandy-gravel quarry N2, which
160 is located near the Nadym–Yagelnoye Road (absolute elevation 50 m). The total thickness of
161 the exposed stratum was estimated as about 421 cm. Detailed descriptions of each horizon
162 and layer of the strata are given in Table 2, and a general view of the section is shown in
163 Figure 2(b).

164 2.2 Methods

165 Samples of sediments were taken from each of the horizons for morphological analyses
166 using grain morphoscopy. The chemical composition and grain size distribution were also
167 identified. The main oxide concentrations using an X-ray fluorescence method and SEM
168 photos were done in Analytical Center for multi-elemental and isotope research of the
169 Sobolev Institute of Geology and Mineralogy of the Siberian Branch of the Russian Academy
170 of Sciences (SB RAS). The grain-size distribution was determined using a dry screening
171 method (a sieving test) with a vibratory sieve shaker (Analysette 3, Fritsch, Germany,
172 [https://www.fritsch.com.ru/podgotovka-prob/rashev/vibracionnye-
173 grokhoty/detali/produkty/analysette-3-spartan/compare/](https://www.fritsch.com.ru/podgotovka-prob/rashev/vibracionnye-grokhoty/detali/produkty/analysette-3-spartan/compare/) (page viewed 04.05.2019)). Fractions
174 were quantified gravimetrically with a precision of 0.1 g.

175 Quartz grains of medium- and coarse-grained sand were studied using a binocular
176 microscope according to the technique developed by the Institute of Geography of the RAS
177 (Velichko & Timireva, 1995). Images of the grains were obtained by scanning electron
178 microscope (Tescan MIRA 3 LMU). The roundness of the grains and their shapes were
179 evaluated according to the method reported by Rukhin (1969) and the 5-grade scale reported
180 by Khabakov (1946). The roundness coefficients and the degree of surface dullness were then
181 calculated for each sample (Velichko & Timireva, 1995). In general, these methods are in
182 good correspondence with the procedure for the preparation of samples described by Krinsley
183 & Doornkamp (1973).

184 The surface shape and heterogeneity of the grains were determined visually on a
185 gradient ranging from glossy to matte. This method was previously used when studying
186 underlying sands under the peat deposits near the Siberian Uvaly, the Taz and Pur Rivers
187



188 (Velichko et al., 2011), and Aeolian sediments in the south of West Siberia (Sizikova &
189 Zykina, 2015).

190 Sampling was also conducted in the lowest horizon of section K-1 for absolute age
191 dating using the optically stimulated luminescence technique (the analysis was performed by
192 N. A. Molodkov at Tallinn University). In total, 15 samples were taken from one of the
193 quarries for further petrographic study (coordinates N65.061368° E72.943045°). The samples
194 were prepared into the form of thin sections in the perpendicular direction with transparent
195 slices. Their micromorphology was then investigated under an optical microscope (Carl Zeiss
196 AxioScope A1, Sobolev Institute of Geology and Mineralogy of the SB RAS, Novosibirsk).

197 Digital terrain models (DTMs) were used to characterize the geomorphic features of the
198 studies sites. This was the first time that this was done for the investigated territory. The
199 DTMs had spatial resolutions of 12 and 26 mpx and were created using satellite images from
200 TerraSAR-X and TanDEM-X. The initial data were obtained within the framework of a
201 research project supported by the Terrasar-X team for the purpose of studying possible
202 applications of the TanDEM DTMs in scientific research (DEM_GEOL1378). Multispectral
203 space images were used (10 mpx), which are generally available thanks to the Sentinel-2
204 mission (Copernicus Open Access Hub, n.d.).
205

206 3. Results

207 3.1. Bulk chemical composition

208 Data about the oxide content are given in table 3. Based on the main oxide
209 concentrations, it is possible to evaluate main differences in sedimentation processes in
210 various paleoenvironments. To clarify the differences of various stages of sedimentation,
211 section K-1 was divided in two sub-layers and sampled. Data on the concentrations of SO₃,
212 V₂O₅, Cr₂O₃, and NiO are omitted because they were lower than the detection limit in all
213 samples.

214 All of the studied layers are characterized by a horizon with a high content of silica
215 oxide. Aluminium and iron oxide were also dominant in the chemical composition of the
216 samples. The silica content was higher in horizon 6, which also had very low contents of
217 aluminium, titanium, magnesium, iron, manganese, calcium, and other elements. Therefore,
218 this horizon can be attributed to oligomictous sands that sustained long-term exposure and
219 could preserve only the most stable mineral, silica.

220 The exposed deposits are part of the second terrace located above the floodplain, and
221 upon first glance, they demonstrate a transition zone from the channel and floodplain facies
222 to a series of subaerial sediments. For horizon 6 of section K-1, absolute age dating was
223 performed using the optically stimulated luminescence (OSL) method. The determined age
224 was 24.3±1.7 thousand years (RLQG 2443-057, U_{ppm}=0,11, Th_{ppm}=0,45, K%=0,01), which
225 corresponds to the interchange from the warm Karginsky Age to the last Sartan Ice Age.
226

227 3.2. Grain size composition

228 The particle size distributions are given in table 4. Horizon 6 of section K-1 clearly
229 demonstrates a predominance of medium- and coarse-grained sand fractions, while finer
230 fractions are in smaller quantities, and silt and clay particles are almost absent. Horizon 6 of
231 section K-2 is also marked by a minimal content of silt and clay and a very high content of
232 medium-grained sand. This could be interpreted as the result of high fluvial velocity and
233 sufficient washing of the sediment matter. In the top sediment layers, the silt and clay content
234 were high, which is characteristic of Aeolian sediments.
235



236 3.3. Morphoscopy of the quartz sand-grains

237 The micromorphology data of the quartz grains are given in table 5. For section K-1, a
238 low roundness coefficient is clearly observed from horizons 2 to 6/2, while the degree of
239 surface dullness drops at horizon 3 and remains within 33-44.5% from horizons 3 to horizon
240 6/2 (Table 5). The coefficients and distribution of the sand grains according to their
241 roundness in the sequence of horizons 1-3 suggest a significant influence of Aeolian
242 processes on the transport of sand. The possible presence of intensive aeoliation is also
243 supported by the morphoscopic data, where grains with micro-pitted texture are observed in
244 the samples, which is an indicator of subaerial impact (Velichko & Timireva, 1995; Vos et
245 al., 2014; Krisley & Doornkamp, 1979).

246 In addition to micro-pitting, signs of fluvial transport are rather distinct (fine-pitted
247 and smooth surfaces, V-shaped pits, and crescentic percussion marks). Therefore, these sand
248 grains were shaped due to the following process: first, they were transported by water flow,
249 and then they were eroded from river valleys and transported by wind for a short distance.
250 This is indicated by the prevailing micro-pitted texture of the protruding edges of the grains.

251 For horizons 4 and 5, high roundness coefficients and low degrees of surface dullness
252 are typical, which is an indicator of significant subaqueous impact. This is also supported by
253 the prevailing number of well-rounded and perfectly rounded grains (Figure 3), as well as the
254 frequency of fine-pitted surfaces and subaqueous V-shaped pits (Vos et al., 2014; Krisley &
255 Doornkamp, 1979). Some grains show the indications of Aeolian processes in the form of
256 micro-pitted texture.

257 In horizons 6/1 and 6/2, glossy grains are notably abundant regardless of the
258 roundness (Figure 3), which suggests aqueous transport. The prevalence of glossy grains
259 among the subangular and perfectly rounded grains (Figure 3) can be attributed to the
260 presence of two washout sources, one of which could have brought in unaltered material.
261 Morphoscopy data also illustrate that the fluvial nature was one of the key factors of this
262 horizon.

263 In terms of roundness, the sand grains from both layers can be divided into two
264 groups. The first group includes grains of grades III and IV, which are often glossy unless
265 damaged by chemical processes, and their main features are fine-pitted surfaces (Figures 4
266 (a)-(d)) and crescentic percussion marks (Figures 4 (a), (d), (f), (h)). Most frequently, these
267 grains are characterized by spherical or nearly spherical shape, which could be connected
268 with long-lasting subaqueous impacts.

269 Group 2 includes sub-angular and sub-rounded grains of irregular shape and smooth
270 surface texture (Figure 3). The main feature of these grains is crescentic pits (Figures 4 (f)-
271 (h)). The ground-down flat faces (Figures 4 (a), (e)) and elongated form (Figures 4 (a), (c))
272 support the idea that the grains were not exposed to subaqueous impact for enough time to
273 obtain a regular shape. Some grains are characterized by various grooves and scratches,
274 which often appear due to intense mechanical alteration, as well as conchoidal fractures
275 (Figures 4 (f), (j)), which are caused by frost weathering. If water or other liquids penetrate a
276 crack and then freeze, the grain splits (Velichko & Timireva, 1995). Such flat faces, grooves,
277 scratches, and fractures have rounded edges, and textures that are typical for aqueous impact
278 can be often detected on them. Therefore, a post-sedimentation origin appears impossible.

279 Presumably, the glacial deposits were washed down the course of the flow that
280 collected and transported part of this material. It should also be noted that the amount of
281 subangular material in horizon 6/2 is higher than in horizon 6/1, which could indicate that
282 during the sedimentation of horizon 6/2, the deposits represented by grains from group 2
283 were washed down more intensively. All horizons of the section were subject to post-
284 sedimentation chemical erosion and frost weathering.



285 According to the morphoscopy data and quartz sand grains from horizons 1–3 in
286 section K-2, we can conclude that both alluvial and Aeolian transport was critical for the
287 formation of these sediments, which is demonstrated by the high roundness coefficients,
288 medium degree of surface dullness (Table 6), and good roundness of the material (Figure 3).
289 Fine-pitted surfaces, crescentic texture, and V-shaped pits are indications of fluvial transport
290 of the sand (Vos et al., 2014; Krinsley & Doornkamp, 1979). Micro-pitting that results from
291 Aeolian transport is found on such marks or on the grain surfaces (Velichko & Timireva,
292 1995).

293 For the content of the grains of subaerial origin in horizons 4 and 5, transport is not
294 high, and the principal factors in the sedimentation of these layers were subaqueous
295 processes. Horizon 6 was also formed by alluvial sedimentation but differs considerably from
296 the above horizons in terms of the sand-grain distribution and prevailing low grades of
297 roundness (Figure 3). Horizon 6 includes a significant number of grains with post-
298 sedimentation conchoidal fractures and flat faces. These features could be related to the flow-
299 collected material being exposed to the frost and mechanical impacts typical of glacial
300 deposits.

301 In general, the morphoscopy of grains from horizon 6 and the mechanism of their
302 sedimentation appear similar to those of layers 6/1 and 6/2 in section K-1. Horizon 6 in both
303 examined sections is distinguished by the morphology of the sand grains. They are
304 characterized by the lowest roundness coefficients (63-65%) and degrees of surface dullness
305 (33-35%, Tables 5 and 6), the presence of the glossy grains at all grades of roundness,
306 smoothed and ground-down flat faces, crescentic texture, and fine-pitting on the surfaces.
307 Based on these characteristics, it can be concluded that horizon 6 was formed by fluvial
308 processes, although it should be noted that it includes material typical of glacial deposits.
309

310 3.4. Petrographic analysis

311 The petrographic analysis of 15 samples taken in section K-2 clearly allowed us to
312 revealed several groups of materials:

313 1) The first group (6 samples) is presented by grey, yellowish-grey, and greenish-grey
314 fine-grained and very fine-grained sandstones and siltstones with slab jointing. They are
315 usually moderately or poorly sorted and have primary foliation that is emphasized by the
316 regular orientation of flattened grains, varying grain size, and matrix content. The matrix is
317 hydromicaceous clay, sometimes with ferruginous cement, with a small portion of silica. The
318 fragments are usually sub-rounded or sub-angular. The rock is composed of polymictic
319 sandstones, similar to arkosic sandstones. Quartz and feldspar prevail among the mineral
320 grains, composing ~30 vol% of the fragments, while another third is predominantly
321 composed of siliceous rock fragments. Some samples contain significant amounts of
322 muscovite (up to 5% by volume), chlorite (including pseudomorphs after the dark-coloured
323 minerals), and epidote. The presence of muscovite could be an indicator of low weathering of
324 initial sediments.

325 2) Pebbles and boulders of the second group of quartzitic and quartz sandstone (6
326 samples) feature angular forms. The textures are usually massive and vary from poorly to
327 well sorted. The cement is predominantly quartz or quartz-hydromicaceous, sometimes with
328 goethite. The grain size varies greatly, but medium-sized varieties prevail. More than 95% of
329 grains are quartz and siliceous lithoclasts, while muscovite, feldspar, epidote, zircon,
330 monazite, and opaque minerals are also present. The quartzitic sandstones show regenerative
331 incrustations around the primary rounded quartz grains. The grain boundaries are most often
332 irregular and frequently saw-shaped, which indicates a notable meta-genetic alternation. Late
333 veins of the fine-grained quartz aggregate are also rather frequent.



334 3) The third group of samples was the least numerous yet the most informative. In this
335 case, the first sample is a cobble of pinkish quartz trachyte–alkaline intermediate volcanic
336 rock. Large pelitized phenocrysts of potassic feldspar (up to 1 cm) and rare fine quartz grains
337 are distributed in the groundmass composed of pelitized potassic feldspar and quartz (Figure
338 5(a)). Furthermore, quartz-feldspathic myrmekites are rather frequent. There are small
339 quantities of plagioclase, dark-coloured minerals that are substituted by aggregates of
340 chlorite, epidote, and opaque mineral.

341 The second sample is dolerite with typical poikilitic texture (Figure 5(b)) formed by
342 large poikilite clinopyroxene crystals (3–4 mm in diameter) with tabular plagioclase (up to 1–
343 1.5 mm). There are large, separate hypidomorphic crystals of basaltic hornblende (up to 2
344 mm), which are substituted by hydrous ferric oxides, titanite, and chlorite. The main
345 groundmass contains plagioclase and significant amounts of chlorite, which is presumably a
346 product of substitution of the volcanic glass or clinopyroxene microliths.

347 The third sample is zoisite-amphibolite (zoisite-actinolite) metasomatic rock. Light-
348 green idiomorphic grains of amphibole prevail over hypidomorphic crystals and sheaf-like
349 aggregates of zoisite. Anhedra segregations of titanite and opaque ore minerals are also
350 present. From a general chemical perspective, it can be suggested that the most probable
351 protolith for this rock was a dolerite-like rock.
352

353 3.5. Relief

354 The study area is located in northern sparse taiga with vast wetlands. Thus, the relief
355 structure was captured in great detail by the DTMs obtained with X-band radar data (with
356 deep penetration capability). Analysis of the recent DTM revealed two typically glacial relief
357 forms, which has been described previously on geological and glaciological maps (Shatsky,
358 Babushkin, 1996; Astakhov et al., 2016):

359 1) An area of the linear-ridged relief is located on the right side of the Yarudei River
360 (left-side tributary of the Nadym River) near the Nadym–Salekhard transportation corridor,
361 which was in process of construction (Figures 1 and 6). Two long, curved mountain ridges
362 rising up to 55 m (the difference in relative elevation is 10–12 m) are well preserved. South of
363 the ridges, there is an area of undulating, presumably kame relief. The ridges are composed of
364 thermocast and erosional forms.

365 2) An area of the kame and easker relief is located on the right side of the Nadym
366 River, south of the gas mainlines (Figures 1 and 7). The kames form a chain of hills rising up
367 to 100 m (the difference in relative elevation is 30 m). The hills are well preserved, despite
368 the fact that some formations were eroded by the fluvial network.

369 The studied areas of presumably glacial relief are located at different
370 geomorphological levels and apparently belong to different ice ages. The good preservation
371 of the relief indicates its stability during the warmer ages and periods of active erosion. In
372 addition, these areas are not covered by marine sediments.

373 4. Discussion

374 Systematic geological studies of the Nadym River Basin began in the late 1940s, and
375 since then, the problem of correlation between glaciations and marine transgressions has been
376 under intensive discussion. Various stratigraphic schemes have been reflected in the state
377 geological maps (<http://webmapget.vsegei.ru/index.html>). For example, map sheet Q-42-43
378 (Shchatsky, 1996) takes into account the complex interrelations between glacial,
379 fluvioglacial, lacustrine-glacial, and marine sediments. However, further south, map sheet P-
380 43 (Kovrigina, 2010) presents the entire variety of Quaternary sediments as steps of marine
381 terraces, completely denying any evidence of glaciation. The marine concept of the territory
382 development has also appeared in derivative works (field reports of a previous expedition).



383 Thus, in detailed relief studies of the basin of the Nadym, Pur, and Polui Rivers, only marine
384 and lacustrine-alluvial deposits were considered as lithological grounds for differentiation of
385 the natural sites (Melnikov et al., 1983).

386 Recent works based on the extensive use of modern dating methods and actual ERS
387 data point to widespread glacial sediments in the entire northern end of West Siberia
388 (Astakhov, 2017). However, opponents of the glacial concept suggest that the glacier could
389 not have filled such vast territories even during the coldest ages (Kuzin, 2013; Sheinkman,
390 2015). It is important to note an intermediate concept of localized (Velichko, 1997) or passive
391 (Bolshiyakov, 2006) glaciation, where separate ice caps were formed on the watersheds
392 instead a solid ice sheet, and the river flow remained unblocked. In this context, the problem
393 of the deposit genesis at local sites could be solved with the help of various geological and
394 geomorphological methods.

395 The most interesting phenomenon in the territory is a layer of supposedly
396 fluvio-glacial deposits, which lies at the base of the second terrace above the flood plain. It
397 stretches vastly in the plane (more than 30 km) and differs significantly from the overlying
398 layers in terms of thickness, lamination, and composition of sediments. The cross lamination
399 and predominance of the medium- and coarse-grained material indicate high flow rates, and
400 the sediments are characterized by a flushing regime, which resulted in poor chemical
401 composition. This layer also contains inclusions of coarse clastic material, but large pebbles
402 with longitudinal dimensions of up to 15-20 cm that occur at the bottom of the quarry were
403 not found in the section.

404 At the base of section K-2, there were well-rounded pebbles of up to 10 cm in size
405 and angular boulders, some of which had a flatiron shape or ground-down flat faces that were
406 either bevelled or parallel to each other. The absolute age of the presumably fluvio-glacial
407 deposits (24 thousand years) allows us to attribute the time of their formation to the late
408 Karginsky interstadial, which corresponds to numerous radiocarbon and OSL datings of the
409 second terrace over the entire northern end of West Siberia (the dating range is from 42 to 25
410 thousand years) (Nazarov, 2015). On average, the age of the cover complex is lower and
411 ranges from 20 to 12 thousand years (Astakhov, 2006; Zemtsov, 1976).

412 The sand quartz grain morphoscopy showed that the grains of this layer came from
413 two different sources. One of the sources could be related to glacial deposits eroded by the
414 water flow. This can be supported by the presence of angular grains with irregular shapes,
415 smooth surfaces, and flat faces. The surfaces of grains often feature various grooves and
416 scratches, which are formed by mechanical impact, and conchoidal fractures, which are the
417 result of frost weathering.

418 Such morphology is typical of fluvio-glacial sediments. Thus, in the Protva river basin
419 in European Russia, Alekseeva (2005) points out “angular grains with sharp or slightly
420 rounded edges and corners. The surface of grains is complicated by large and small chips
421 with conchoidal fractures. Many grains have scratches and parallel striae in the fractures,
422 which is characteristic of glacial grains”. According to Krinsley and Doornkamp (1973, p.
423 44-50), the same features (irregular curved shape, ground-down flat faces, and conchoidal
424 fractures) are present on the grains from present-day Swiss glaciers, and sub-rounded and
425 fine-pitted grains from a fjord delta are also located on the margin of a present-day glacier in
426 Norway.

427 The subaerial origin of horizons 1–2 and the prevailing aqueous environment during
428 sedimentation of horizons 3–5 in the sections correspond to the results obtained by Velichko
429 et al. (2011). They studied of grains from the sands underlying peat bog deposits in the same
430 territory. In addition, they point to angular grains with a low degree of surface dullness,
431 which were discovered near the town of Noyabrsk and in the Pur River basin. These grain
432 features are associated with glacial-marine sediments.



433 The petrographic diversity of erratic boulders in West Siberia allows us to distinguish
434 two or three paleoglacial regions that unite several dozen distributed provinces, each of which
435 is characterized by a definite set of rocks and petrographic features. The first major
436 generalization in this respect was made by Zemtsov (1976), who identified the guide boulders
437 of the Ural region as ultramafic and mafic rocks of the Main (axial) Uralian zone, plagiogranites,
438 and highly metamorphosed rocks (gneisses and shales). In the Central Siberian
439 region, the prevailing boulders include dolerites and basalts of the Putorana Plateau, as well
440 as various granitoids, quartzites, and Paleozoic sandstones of the Taimyr Region. These
441 studies were substantially supplemented and detailed by a much more ambitious work by
442 Sukhorukova et al. (1987).

443 Despite their small quantity, the petrographic analysis of pebbles and boulders
444 sampled in quarry N2 led to the following conclusions. Firstly, high-silica alkaline effusive
445 rocks (sample H-10, quartz trachyte) are indicative of both the Northern Taimyr Province
446 (Troitsky & Shumilova, 1973) and many moraines of the Ural paleoglacial region
447 (Sukhorukova et al., 1987), but they are never found in the Putorana Plateau and more
448 southern regions. Moreover, there were only a small relative proportion of dolerites (sample
449 H-14, dolerite) and other effusive mafic rocks, which are characteristic of Putorana and
450 Nizhnyaya Tunguska regions. In contrast, there are no limestones that would be typical of the
451 Central Siberian paleoglacial region (the Kulyumbinsk and Sukhaya Tunguska distributive
452 provinces according to Sukhorukova et al., 1987). However, there are also no granites in the
453 sample that are characteristic of the Northern Taimyr region.

454 Secondly, quartz and quartzitic sandstones are typical for the Ural paleoglacial region,
455 but their share is usually within a few per cent. Quartzitic sandstones also described as
456 Paleozoic were found 50 km north of Surgut within the tentative Central Siberian and Middle
457 material outwash zones (Sukhorukova et al., 1987). The source of polymictic platy jointing
458 sandstones could be the Paleozoic bordering of the eastern slope of the Urals (Sukhorukova et
459 al., 1987) or the Mesozoic sandstones of the West Siberian Plate.

460 In general, the samples have a significant proportion of terrigenous rocks (sandstones
461 and siltstones) and a low content of dolerites. On the one hand, this can be explained by poor
462 representativeness of the samples. Nevertheless, the main zone of material washout could be
463 located further north than the Putorana Plateau in the Taimyr area. In order to substantiate
464 this point of view, further research is planned to determine the trace element composition and
465 absolute dating and to expand the sampling.

466 The linear-ridged relief formed as a result of glacial impact in the north of West
467 Siberia is marked on the Map of Quaternary Formations of Russia at a scale of 1:2,500,000
468 (Astakhov, 2016). In addition, the linear forms and glacial remains are marked on geological
469 maps at larger scales, such as Map Sheet Q-42 (Zyleva et al., 2014). Detailed aerial
470 photographs and space images of medium spatial resolution have often been used for the
471 purposes of mapping the relief. However, the methodology for determining the glacial
472 genesis was rather poor, and DTMs were not used much.

473 At the present stage, the most promising approach seems to be the use of DTMs
474 obtained by radar interferometric and optical stereoscopic photography. In combination with
475 high-resolution images under the conditions of sparse forest vegetation, it becomes possible
476 to map the typical glacial forms in detail using methods that have already been verified in
477 other areas of glaciation (Ely, 2016). In some areas, analysis of the DTMs obtained by the
478 Tandem-X satellite identified dense forestation, a predominance of erosion processes, and
479 well-preserved glacial forms, despite the plain relief of the territory. This is supported by
480 large-scale field studies on the left side of the Levaya Khetta River (Vasiliev, 2007). These
481 studies revealed two types of areas of the glacial relief and extensive sandurs on the surface
482 of the second terrace above the floodplain.



483 The zones of active modern Aeolian processes gravitate toward the sandur areas. It
484 appears that the Aeolian relief occupied significantly larger areas in the north of West Siberia
485 at the end of the Pleistocene Age. This is supported by the detailed studies of quartz grains
486 from near-surface sediments that were carried out in the territory in the early 2000s.
487 (Velichko et al., 2011).

488 DTMs and satellite images of the entire territory provided an opportunity to analyse it
489 from the perspective of landscape indications of the sites exposed to glaciation. In this
490 respect, the vast lacustrine-alluvial plains that reach their maximum area in the basins of the
491 Nadym, Pur, and Taz Rivers can be considered as postglacial sites. Such an assumption,
492 which was first made by Sacks (1940) for the lower reached of the Yenisei River, thus
493 receives new factual support.

494 5. Conclusion

495 This research has shown that the integration of surface techniques and remote-sensing
496 methods is highly efficient for analysing the Quaternary history of sediments that have
497 formed in a region with a complicated geomorphological history and possible glaciation. The
498 sediments of the high bank of the Nadym River can be attributed to fluvio-glacial deposits for
499 a number of reasons. The glacial impact resulted in indicative marks such as linear ridges and
500 kame hills on the relief of certain natural sites in the territory.

501 Thus, it can be concluded that continental glaciation evidently occurred during the
502 Pleistocene Age in the history of the development of the lower course of the Nadym River. It
503 is difficult to conclude whether there was a common ice sheet or if there were several isolated
504 centers of ice accumulation. The available data, especially the relief character on the DTMs,
505 support the second option, at least in the late Pleistocene Age. There may be traces of more
506 extensive glaciations in earlier ages in the extensive lacustrine-alluvial plains, which reach
507 their maximum area in the basins of the Nadym, Pur, and Taz Rivers. In this case, they can be
508 considered as postglacial sites that later underwent erosion transformations but retained the
509 characteristic structure inherited by present-day landscapes.

510 Acknowledgements

511 We thank the Terrasar-X team (DLR) for the provided DTMs. This research was
512 supported by the joint grant of the Russian Foundation for Basic Research and the
513 Government of Yamalo-Nenets Autonomous Okrug (No. 16-45-890529 p_a) and state
514 assignment of IGM SB RAS funded by Ministry of Science and Higher Education of the
515 Russian Federation.

516 References

- 517 Alekseeva, V.A.: Micromorphology of quartz grain surface as indicator of glacial
518 sedimentation conditions: evidence from the Protva River basin, *Lithology and Mineral
519 Resources*, 40(5), 420-428, 2005.
- 520 Alyavdin F. and Mokin N.P.: Map sheet Q-43 - New Port. Geological map]. Cartographic
521 factory of Gosgeoltekhizdat of the Ministry of Geology and Subsoil Protection of the
522 USSR. Available at: <http://webmapget.vsegei.ru/index.html>, 1957.
- 523 Astakhov, V.I.: On chronostratigraphic units of the Upper Pleistocene in Siberia, *Geologiya i
524 geofizika*, 47(11), 1207-1220, 2006.
- 525 Astakhov V. Shkatova V., Zastrozhnov, A. and Chuyko, M.: Glacio-morphological Map of
526 the Russian Federation, *Quaternary International*, 420, 4-14, 2016.
- 527 Babushkin, A.E. Quaternary map. 2nd ed. Scale 1:1,000,000. Russian Federation Committee
528 on Geology and Mining (Roskomnedra), Map Q-42,43 (Salekhard). St. Petersburg:
529 VSEGEI Cartographic Factory, 1995.



- 530
531 Bolshiyarov, D.Yu.: Passive Glaciation of the Arctic and Antarctic Regions. AANII, Saint
532 Petersburg., 296 p, 2006.
533 Copernicus Open Access Hub (n.d). Available at: <https://scihub.copernicus.eu/dhus/#/home>
534 Ely, J., Gribble, E. & Clark, C.D.: The glacial geomorphology of the western cordilleran ice
535 sheet and Ahklun ice cap, Southern Alaska, Journal of Maps, 12(sup1), 415-424, 2016
536 Faibusovic, Ya. E. and Abakumov, L.A.: Map sheet Q-43 - New Urengoy. Map of Pliocene-
537 Quaternary formations. Sheet 1. VSEGEI Cartographic Factory, St. Petersburg.
538 Available at: [http://www.vsegei.ru/ru/ru/info/pub_ggk1000-3/Zapadno-Sibirskaya/q-](http://www.vsegei.ru/ru/ru/info/pub_ggk1000-3/Zapadno-Sibirskaya/q-43.php)
539 [43.php](http://www.vsegei.ru/ru/ru/info/pub_ggk1000-3/Zapadno-Sibirskaya/q-43.php), 2015.
540 Fredin, O., Rubensdotter L., Welden, A., Larsen, E. and Lysa, A.: Distribution of ice
541 marginal moraines in NW Russian, Journal of Maps, 8(3), 236–241, 2012. doi:
542 10.1080/17445647.2012.708536
543 Generalov, P.P.: Upper Pleistocene of the lower course of the Ob River In: Collection of
544 scientific papers of the West Siberian Scientific and Research Geological Prospecting
545 Petroleum Institute, Tyumen, 56-77, 1986.
546 Generalov, P.P.: Legend to Tyumen-Salekhard subseries of Western Siberia series of sheets
547 of the State Geological Map of RF at scale of 1:200000. In: Report of West Siberian
548 Geological Research and Analytical Center, Tyumen, 1998.
549 Grosvald, M.G.: Eurasian Hydrospheric Catastrophes and Glaciations of the Arctic Region,
550 Nauchny Mir, Moscow, 1999.
551 Khabakov, A.V.: On roundness indexes of pebble, Sovetskaya Geologiya, 10, 98-99, 1946.
552 Kovrigina, E.K. (Ed.) Map sheet P-43 – Surgut (the Third Generation). Explanatory Note.
553 Saint-Petersburg, VSEGEI Cartographic Factory, 2010.
554 Krinsley, D. H. and Doorkamp, J. C.: *Atlas of Quartz Sand Surface Textures.*, Cambridge
555 University Press, Cambridge, 1973.
556 Kuzin, I.L.: Myths and Reality of the Theory of Continental Glaciations, Nasledie, Saint
557 Petersburg, 2013.
558 Lazukov, G.I.: Antopogen of the northern part of Western Siberia (Paleogeography). M., 127
559 p, 1972.
560 Maslennikov, V.V.: Regional Geo-Ecological Mapping at Scale of 1:1000000 Within the
561 North End of Tyumen Oblast. Labytangi, 1998.
562 Melnikov, E.S., Weisman, L.I. and Moskalenko, N.G. (Eds.): Landscapes of criolithic zone
563 of the West Siberian gas bearing province. Nauka, Novosibirsk, 1983.
564 Nazarov, D.V.: Upper Pleistocene in the northern end of Western Siberia. In: Fundamental
565 problems of the Quaternary, results of the study and the main trends of further
566 research: Proceeding of the IX All-Russian Conference on Quaternary Research
567 (Irkutsk, 15-20 September 2015)], pp. 323-325. Sochava Institute of Geography of the
568 SB RAS, Irkutsk, 2015.
569 Rukhin, L.B.: *Fundamentals of Lithology. Doctrine of Sedimentary Rocks.* Nedra, Leningrad,
570 1969.
571 Rusakov, A., Sedov, S., Sheinkman, V., Dobrynin, D., Zinovyev, E., Trofimova, S. and
572 Levchenko, S.: Late Pleistocene paleosols in the extra-glacial regions of Northwestern
573 Eurasia: Pedogenesis, post-pedogenic transformation, paleoenvironmental inferences.
574 Quaternary International. 501, 174-192, doi:10.1016/j.quaint.2018.03.020, 2018.
575 Sacks, V.N.: Some data on permafrost in the lower course of the Yenisei River. Problemy
576 Arktiki, 1, 62-79, 1940
577 Sedov, S., Rusakov, A., Sheinkman, V., and Korkka, M.: MIS3 paleosols in the center-north
578 of Eastern Europe and Western Siberia: Reductomorphic pedogenesis conditioned by
579 permafrost? Catena, 146, 38–47, doi:10.1016/j.catena.2016.03.022, 2016.



- 580 .Shatsky, S.B. and Babushkin, A.E. (Eds.): Map Sheet Q-42,43 – Salekhard (New Series).
581 Explanatory Note. VSEGEI Publishing House, Saint-Petersburg, 1996.
- 582 Sheinkman V.S. and Plyusnin, V.M.: Glaciation of the northern end of Western Siberia —
583 controversial issues and ways to solve them. *Lyod i Sneg*, 1(129), 103-120, 2015.
- 584 Sheinkman, V., Sedov, S., Shumilovskikh, L., Korkina, E., Korkin, S., Zinovyev, E. and
585 Golyeva, A.: First results from the Late Pleistocene paleosols in northern Western
586 Siberia: Implications for pedogenesis and landscape evolution at the end of MIS3.
587 *Quaternary International*, 418, 132–146, doi:10.1016/j.quaint.2015.12.095, 2016.
- 588 Sizikova, A.O. and Zykina V.S.: The dynamics of the Late Pleistocene loess formation,
589 Lozhok section, Ob loess Plateau, SW Siberia. *Quaternary International*, 365, 4-14,
590 2015.
- 591 Sukhorukova, S.S., Kostyuk M.A., Podsosova, L.L., Babushkon A.E., Zolnikov, I.D.,
592 Abramova, S.A. and Goncharov, S.V. : Moraines and Dynamics of Glaciation in
593 Western Siberia. Works of Institute of Geology and Geochemistry of the Siberian
594 Branch of the USSR Academy of Sciences, Issue 672. Nauka, Novosibirsk, 1987.
- 595 Svendsen, J.I., Alexanderson, H., Astakhov, V.I., Demidov, I., Dowdeswell J.A., Funder S., :
596 Late Quaternary ice sheet history of Northern Eurasia. *Quaternary Science Reviews*, 23
597 (11-13), 1229-1271, 2004.
- 598 Troitskiy, S.L. and Shumilova, E.V.: Stratigraphy and Mineralogical-Petrographic
599 Peculiarities of Quaternary Deposits in the Vorontsov Yar Stratum in the Lower Course
600 of the Yenisei River. In: *Lithology and Conditions of Formation of the Quaternary
601 Deposits of the Northern Eurasia*, pp. 5-37. Institute of Geology and Geochemistry of
602 the Siberian Branch of the USSR Academy of Sciences, Novosibirsk, 1974.
- 603 Vasilyev, S.V.: *Forest and Bog Landscapes of Western Siberia*. Izdatelstvo NTL, Tomsk,
604 2007.
- 605 Velichko, A.A.: Current state of conceptions on continental glaciers of the Earth. *Bulletin of
606 the Academy of Sciences of the USSR, Geographical Series*, 3, 21-34, 1987.
- 607 Velichko, A.A. and Timireva S.N.: Morphoscopy and morphometry of quartz grains from
608 loess and buried soil layers, *GeoJournal*, 36(2/3), 143-149, 1995.
- 609 Velichko, A.A., Kononov, V.M. and Faustova M.A.: The last glaciation of Earth: size and
610 volume of ice-sheets, *Quaternary International*, 41 (42), 43-51, 1997.
- 611 Velichko, A.A., Timireva, S.N., Kremenetski, K.V., McDonald, G.M. and Smith, L.C.: West
612 Siberian Plain as a late glacial desert, *Quaternary International*, 237 (1-2), 45-53, 2011.
- 613 Vos, K., Vandenberghe, N. and Elesen, J.: Surface textural analysis of quartz grains by
614 scanning electron microscopy (SEM): From sample preparation to environmental
615 interpretation, *Earth-Science Reviews*, 128, 93-104, 2014.
- 616 Zastrozhnov, A.S., Shkatova, V.K., Minina, E.A., Ternogradskiy, V.D., Krutkina, O.N.,
617 Krasotkin, S.I. and Gusev, E.A.: A new map of the quaternary sediment of the Russian
618 Federation. 1:2 500 000, Proceedings of VII All-Russia congress on investigation of the
619 Quaternary period. Apatity. Vol. 1. p. 209-211, 2011.
- 620 Zemtsov, A.A.: *Geomorphology of the West Siberian Plain (Northern and Central Parts)*,
621 Publishing house of the Tomsk State University, Tomsk, 1976.
- 622
623
624
625
626
627
628
629



630 **Table Legends**

631

632 Table 1. Description of section K-1

633 Table 2. Description of section K-2

634 Table 3. Total content of oxides in the sections (wt.%)

635 Table 4. Grain-size composition of the studied sections

636 Table 5. Morphometric properties of the quartz sand-grains from section K-1

637 Table 6. Morphometric properties of the quartz sand-grains from section K-2

638

639

640 **Figure legends**

641

642 Figure 1. Location map, where 1 is the area of linear-ridged relief; 2 is the area of kame
643 relief; K-1 and K-2 indicate section K-1 and K-2, respectively (by TanDEM©DLR)

644 Figure 2. Sections K-1 (a) and K-2 (b), photo by Sizov O.S., 2016

645 Figure 3. Distribution of quartz sand-grains from section K-1 (a) and section K-2 (b)
646 according to their roundness and dullness, where 1 is glossy, 2 is quarter-matted, 3 is half-
647 matted, 4 is matted; 0, I, II, III, IV are grades of roundness according to the scale of
648 Khabakov (1946)

649 Figure 4. Pictures of quartz grains from horizon 6/2 section K-1: (a) glossy grain with smooth
650 surface and flat faces; the faces feature crescentic pits, grain tops feature fine pits; (b) fine-
651 pitted surface of grain 'a'; (c) glossy grain with smooth surface and sparse fine pits; (d) half-
652 matted grain with fine-pitted surface and crescent pits; (e) glossy grain with flat faces and no
653 evident texture; (f) glossy grain with post-sedimentation conchoidal fractures and crescentic
654 pits; (j) conchoidal fracture of grain 'e'; (h) crescentic texture of grain 'e'.

655 Figure 5. (a) Sample N-10 – pinkish quartz trachyte, large inclusions of potassic feldspar
656 (Kfs) with fine quartz grains (Qu) in the quartz-feldspathic matrix; (b) sample N-14 –
657 greenish-brown dolerite, large poikilitic clinopyroxene crystals (Cpx) with thin plagioclase
658 crystals (Pl), in the groundmass – plagioclase chlorite (Chl).

659 Figure 6. Area of the linear-ridged relief, DTM by TanDEM-X, 26 m/px. Map provided by O.
660 Sizov.

661 Figure 7. Area of the kame relief, DTM by TanDEM-X, 26 m/px. Map provided by O. Sizov.

662

663

664

665

666

667

668

669 Table 1
670

Layer	Thickness (cm)	Description
1	15	Podzolic horizon, ashy fine-grained sand, clear transition
2	35	Rusty horizon, fine-grained brown sand, unstratified, diffuse transition
3	111	Illuvial horizon, Aeolian sediments, fine-grained light-brown sand, cross-stratified, gradual transition
4	52	Alluvial horizon 1, cross-stratified, grey-brown, medium- and fine-grained, ferruginous, indications of cryoturbation, diffuse transition
5	47	Alluvial horizon 2, channel facies, parallelly stratified, grey-blue, indications of minor cryoturbation, ferruginous layers available, medium- and fine-grained sand, clear transition
6	175	Fluvioglacial (presumably) horizon, thick, gray-blue, clear transition, cross inter-layers of coarse-grained material are visible, from (upper) unstratified to (lower) cross-stratified, coarse-grained, no indications of cryoturbation, no wedges, ferruginous inter-layers available, coarse pebbles (angular, scratched) occur

671
672



673
674 Table 2.
675

Layer	Thickness (cm)	Description
0	18	Anthropogenic subsoil (removed overburden)
1	16	Podzolic horizon, thin, heterogeneous
2	94	Rusty horizon with cryoturbation and clay inclusions
3	66	Aeolian horizon, cryoturbated, unstratified or indistinctly stratified
4	79	Alluvial horizon 1, whitish, parallelly stratified, ferruginous
5	48	Alluvial horizon 2, channel facies, distinctly stratified, clay inclusions
6	100	Fluvioglacial (presumably) horizon, ferruginous, cross-stratified, pebbles available

676
677

678
 679 Table 3.
 680

Sample	SiO ₂	TiO ₂	Al ₂ O ₃	Fe ₂ O ₃	MnO	MgO	CaO	Na ₂ O	K ₂ O	P ₂ O ₅	BaO
Section K-1											
Layer 1	87.65	0.64	5.27	0.95	0.03	0.18	0.51	1.00	1.66	0.03	0.06
Layer 2	88.09	0.53	5.14	1.89	0.03	0.29	0.32	0.56	1.14	0.05	0.04
Layer 3	89.49	0.41	4.93	1.20	0.03	0.25	0.41	0.75	1.52	0.04	0.06
Layer 4	92.97	0.21	3.35	0.61	0.02	0.11	0.27	0.51	1.32	0.02	0.05
Layer 5	90.71	0.39	4.21	0.92	0.02	0.21	0.38	0.64	1.35	0.03	0.05
Layer 6/1	98.02	0.10	0.88	0.30	0.01	0.06	0.10	0.07	0.25	0.01	0.01
Layer 6/2	98.39	0.08	0.69	0.25	0.01	0.06	0.08	<0.05	0.20	0.01	0.01
Section K-2											
Layer 1	94.35	0.36	2.37	0.47	0.01	0.08	0.19	0.34	0.89	0.02	0.03
Layer 2	94.42	0.21	2.36	0.76	0.01	0.10	0.17	0.27	0.83	0.02	0.03
Layer 3	84.75	0.57	7.44	1.00	0.02	0.26	0.56	1.51	2.38	0.02	0.08
Layer 4	94.99	0.24	2.29	0.40	0.01	0.07	0.15	0.29	0.91	0.02	0.04
Layer 5	90.95	0.51	4.31	1.19	0.03	0.23	0.26	0.45	1.16	0.04	0.05
Layer 6	96.88	0.13	1.23	0.26	0.01	0.06	0.10	0.12	0.49	0.01	0.02

681
 682

683
 684
 685

Table 4.

Layer	Fraction size (µm) / Content (%)					
	very coarse-grained sand 1000-2000	coarse-grained sand 500-1000	medium-grained sand 250-500	fine-grained sand 125-250	very fine-grained sand 90-125	silt/clay <90
Section K-1						
Layer 1	0.08	0.73	9.51	28.74	29.24	31.70
Layer 2	0.30	4.20	32.19	32.08	12.54	18.70
Layer 3	0.06	1.20	11.92	35.61	32.29	18.92
Layer 4	0.04	0.95	16.39	56.70	20.06	5.86
Layer 5	0.03	1.58	19.75	59.89	13.12	5.62
Layer 6/1	1.93	23.75	71.53	1.78	0.45	0.56
Layer 6/2	1.73	46.89	46.27	4.21	0.45	0.45
Section K-2						
Layer 1	0.07	2.26	33.79	37.24	5.47	21.16
Layer 2	0.24	3.32	29.47	54.56	7.12	5.29
Layer 3	0.23	4.51	12.57	13.50	12.23	56.96
Layer 4	0.55	10.31	48.75	32.64	4.31	3.44
Layer 5	2.20	15.56	43.55	27.40	4.87	6.42
Layer 6	0.21	5.38	61.21	27.57	3.72	1.92

686
 687



688
689 Table 5.
690

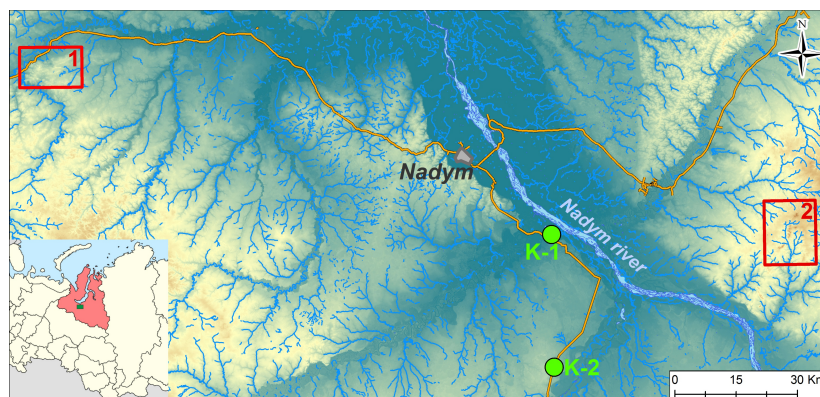
Layer	Roundness coefficient (Q), %	Degree of surface dullness (Cm), %
Layer 1	66.5	61
Layer 2	89	80
Layer 3	83.5	44.5
Layer 4	76	44
Layer 5	73.5	38.5
Layer 6/1	70.5	28.5
Layer 6/2	65	33

691
692

693
694 Table 6.
695

Layer	Roundness coefficient, Q (%)	Degree of surface dullness, Cm (%)
Layer 1	84	47
Layer 2	81	59.5
Layer 3	55.5	52
Layer 4	66	46
Layer 5	70	36.5
Layer 6	63	35

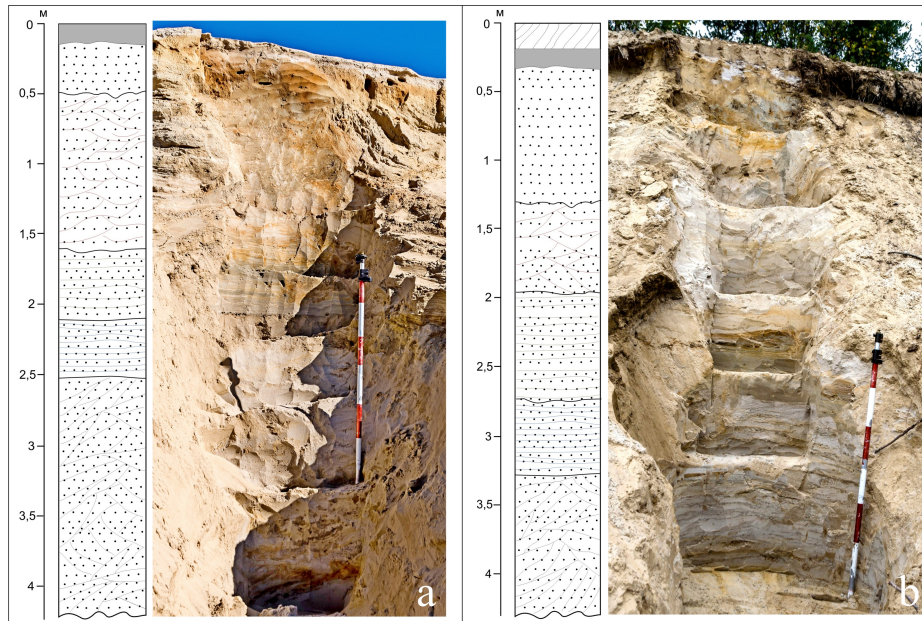
696
697



698
699
700
701
702
703

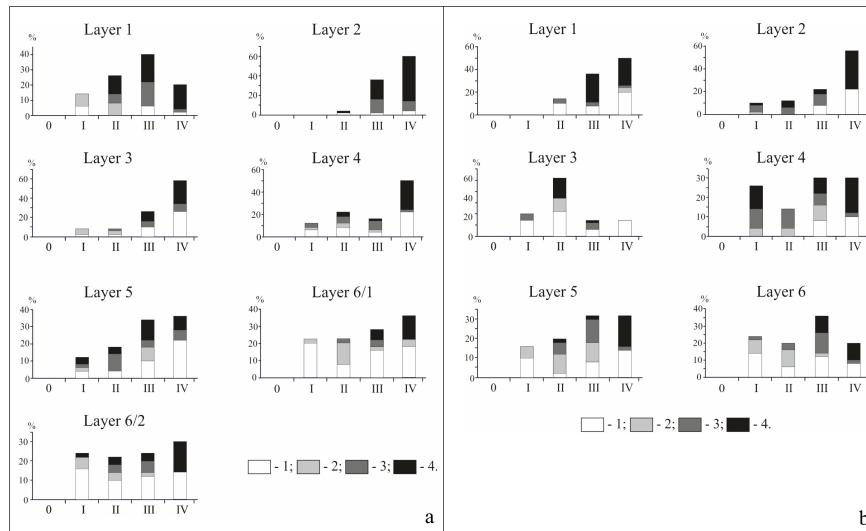
Figure 1. Location map, where 1 is the area of linear-ridged relief; 2 is the area of kame relief; K-1 and K-2 indicate section K-1 and K-2, respectively (by TanDEM©DLR)

704
705



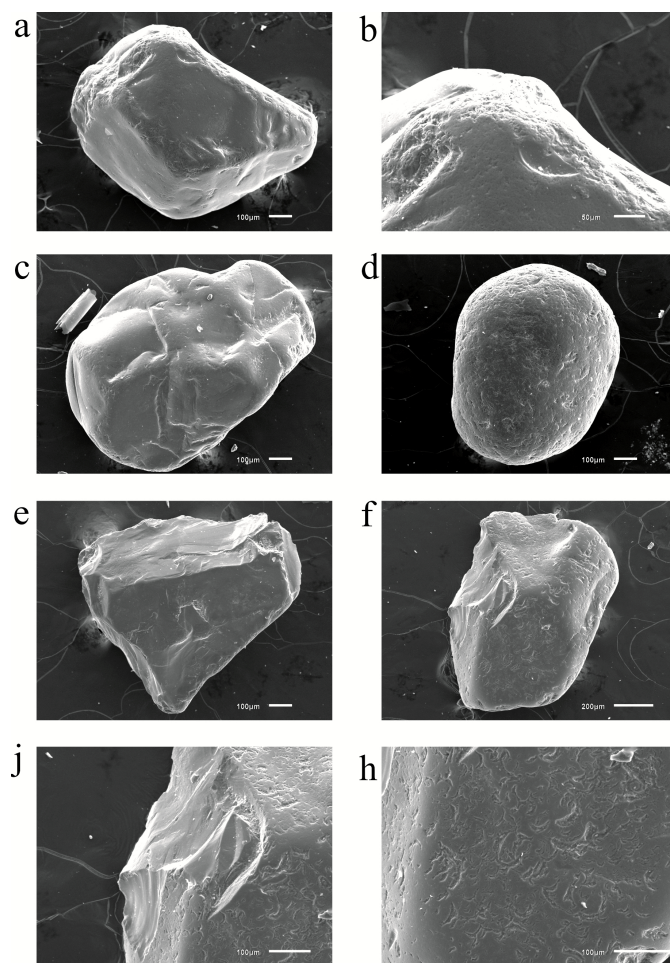
706
707
708
709
710

Figure 2. Sections K-1 (a) and K-2 (b), photo by Sizov O.S., 2016



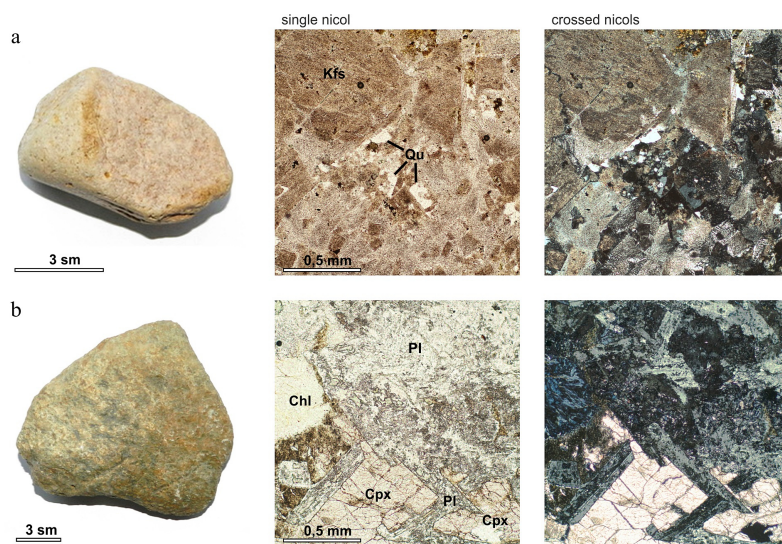
711
 712
 713
 714
 715
 716
 717
 718
 719

Figure 3. Distribution of quartz sand-grains from section K-1 (a) and section K-2 (b) according to their roundness and dullness, where 1 is glossy, 2 is quater-matted, 3 is half-matted, 4 is matted; 0, I, II, III, IV are grades of roundness according to the scale of Khabakov (1946)



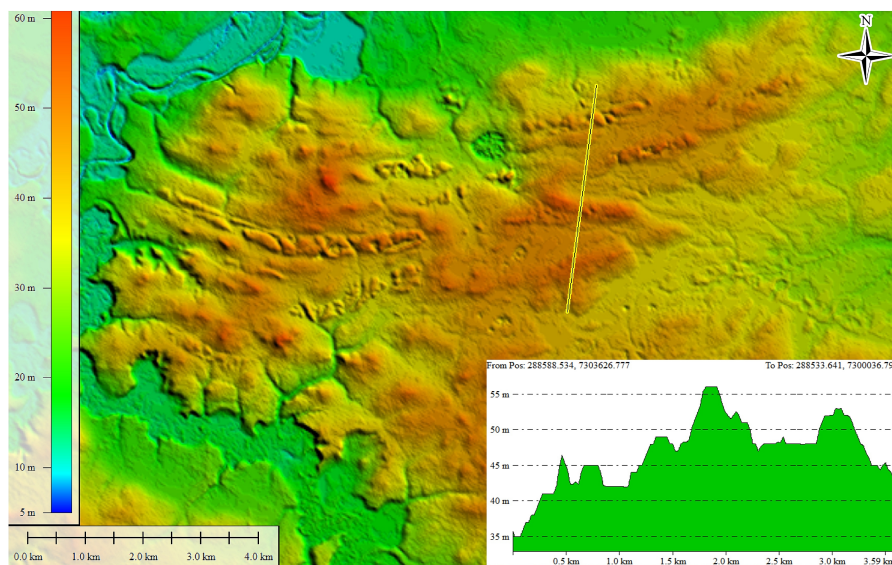
720
721
722
723
724
725
726
727
728
729

Figure 4. Pictures of quartz grains from horizon 6/2 section K-1: (a) glossy grain with smooth surface and flat faces; the faces feature crescentic pits, grain tops feature fine pits; (b) fine-pitted surface of grain 'a'; (c) glossy grain with smooth surface and sparse fine pits; (d) half-matted grain with fine-pitted surface and crescent pits; (e) glossy grain with flat faces and no evident texture; (f) glossy grain with post-sedimentation conchoidal fractures and crescentic pits; (j) conchoidal fracture of grain 'e'; (h) crescentic texture of grain 'e'.



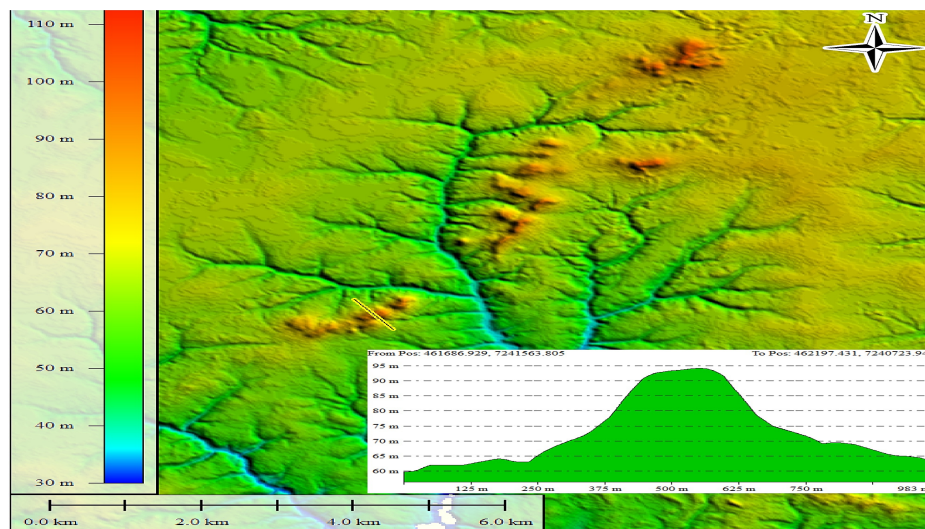
730
731
732
733
734
735
736
737

Fig. 5. (a) Sample N-10 – pinkish quartz trachyte, large inclusions of potassic feldspar (Kfs) with fine quartz grains (Qu) in the quartz-feldspathic matrix; (b) sample N-14 – greenish-brown dolerite, large poikilitic clinopyroxene crystals (Cpx) with thin plagioclase crystals (Pl), in the groundmass – plagioclase chlorite (Chl).



738
739
740
741
742
743

Figure 6. Area of the linear-ridged relief, DTM by TanDEM-X, 26 m/px. Map provided by O. Sizov.



744
745
746
747

Figure 7. Area of the kame relief, DTM by TanDEM-X, 26 m/px. Map provided by O. Sizov.